Determination and investigation of asteroid Apophis' trajectories set potentially colliding with the Earth in 2036

Determination and investigation of asteroid Apophis′ trajectories set potentially colliding with the Earth in 2036

Peng Guo[1], V V Ivashkin[1, 2], C A Stikhno[2] and P M Shkapov[2]

[1] Keldysh Institute of Applied Mathematics, RAS, Moscow, Russia
[2] Bauman Moscow State Technical University, Moscow, Russia
E-mail: ivashkin@keldysh.ru

Abstract. In the paper, we have computed a set of the asteroid Apophis' trajectories, which potentially result in the collisions with the Earth in 2036. Using the developed method and algorithms for determination of these collision trajectories and their impact points on the surface of the Earth, we have obtained its possible impact's path of risk on the world map. We have studied the characteristics in energy, impact time and geometry for these Apophis' trajectories and this impact area. Comparison with results of other authors on this issue shows that they coincide well enough.

1. Introduction

Asteroid (99942) Apophis is well known as one of the most hazardous near-Earth asteroids (NEA) in recent years. Since its first discovery by R. Tucker, D. Tholen and F. Bernardi on June 19, 2004, determination of its initial orbit with the use of optical and radar measurements, estimation of its Earth-impact probability in 2029 and also in the next several decades due to resonant return to the Earth have been studied in many works with different methods. It is shown that Apophis will pass close to the Earth at a distance about 38000 km from the Earth's center on April 13, 2029 and has a low possibility to pass through a "keyhole" about 600 m wide on the target plane of the close encounter, which will lead to a resonant return collision on April 13, 2036 [1–19].

In 2006, Schweickart et al. from the B612 foundation made estimates of the Apophis's possible impact path of risk (PoR) for 2036 [3]. It is shown that the impact PoR extends across many national borders, such as Russia, Nicaragua, Costa Rica, Colombia, Venezuela, etc. In our previous works [6–9] the characteristics of the possible prevention of collision with the Earth and correction of the Apophis' orbit were analyzed. Using the standard ORBFIT software package, Włodarczyk I. computed impact solutions of Apophis up to 2110 based on new observations in 2007 and 2013 and presented the possible impact path of risk for 2036, 2068, 2099 and 2102 [11–13]. Sokolov et al. [14–16] obtained potential impact trajectories of Apophis in the 21st century and investigated the characteristics of potential collisions (the minimum geocentric distance, the relative position of the semimajor axes of the keyholes at the initial time in 2006 and the dimensions of the keyholes).

The purpose of our study is to determine and investigate characteristics of collision trajectories of Apophis and its possible impact area on the Earth's surface in 2036 based on the initial orbit and its uncertainty estimated by IAA RAS in 2005 [1]. This work is an extension of our previous work [10].

This task has been solved in the next two stages. Firstly, we have developed algorithms to search for all set of the Apophis' impact trajectories [6–10]. For this, we have found several sets of impact trajectories, for each of which the perigee distance of orbit is close to some fixed values from the range

$$r_\pi=\{2069\div2100;\ 2500\pm1;\ 3000\pm1;\ldots;\ 6360\pm1;\ 6375\pm1\}\ \text{km}. \quad (1)$$

Secondly, we have determined the intersection points of these trajectories with the Earth's surface. Based on this, we have built the impact path of risk on the world map. We have studied some geometric, temporal and energy characteristics of the Apophis' collision trajectories and the impact area on the Earth, in particular, its width and length, angle of entry into the atmosphere, the time and speed of collision, and also the direction of the asteroid's approach to the Earth.

2. Determination of the asteroid (99942) Apophis' impact trajectories set

2.1. The initial orbital parameters and dynamical model of Apophis

The orbit of the asteroid (99942) Apophis was computed by numerically integrating the differential equations of N-body motion model of Apophis in the heliocentric geoequatorial non-rotational coordinate system OXYZ at the J2000 epoch. In order to improve the accuracy of determining the trajectory of the asteroid Apophis, we have taken into account several perturbations, including the Newtonian attraction of the planets, the Moon and Pluto, as well as the solar radiation pressure, and the Earth's oblateness-J2. The celestial bodies' positions have been computed using the JPL planetary Ephemerides DE405. The influence of relativistic effects and Yarkovsky effect has been ignored in this work. The integration has been performed by the 8th order predictor-corrector method [20].

As the nominal initial parameters, we used the position vector $\mathbf{r}_n$ and velocity vector $\mathbf{v}_n$ of the asteroid and their 3σ uncertainties at epoch t_0: Jan. 30 2005=JD 2453400.5, which were previously estimated by IAA RAS based on optical and radar observations in 2005 [1]:

$$3\sigma_0(x, y, z)=3\ \text{km},\ 3\sigma_0(v_x, v_y, v_z)=2\ \text{mm/s}. \quad (2)$$

Here, in (2), $\sigma_0(x, y, z)$, $\sigma_0(v_x, v_y, v_z)$ are the standard deviations of the components of initial position vector and velocity of the asteroid.

2.2. Search for potential impact trajectories of Apophis

In order to find impact trajectories of Apophis as completely as possible in an acceptable time period and without going through the entire region of initial state due to uncertainties (2) by a very small step, we have created the fast and effective algorithms to search for several sets of trajectories with given values of the perigee distance r_π based on the Monte Carlo and gradient descent methods, which include the following six stages [6–10]:

1) To find a small number (~ 50) of the asteroid's trajectories with minimum geocentric distance less than about 5 million km for the 2036 encounter by Monte Carlo method in the uncertainty region of initial state;

2) By varying the initial states of these trajectories, we perform descent (decreasing the geocentric perigee distance r_π) to trajectories, which will lead to collision with the Earth in 2036, when r_π is less than the Earth's mean radius. Figure 1 shows this search process for one impact trajectory by the gradient descent method;

3) To compute the range of the heliocentric energy constant h_0 of the two-body system at the epoch t_0 for these found collision trajectories of Apophis. Energy depends on the solar gravitational parameter μ_S, the initial heliocentric distance r_0 and speed v_0:

$$h_0 = v_0^2 - 2\mu_S / r_0\ ; \quad (3)$$

4) To applicate the exhaustive method to search for impact trajectories from about 10 million ones, whose energy constants h_0 at t_0 are close to those of collision trajectories. After that, we will find about

20 000 additional impact trajectories, whose energy constants enter into the indicated range (Integration from epoch t_0 to the encounter in 2036 was performed only if the energy constant did not go far away from this range);

5) For each of these additional impact trajectories, we perform descent again, like in stage 2, to find more impact trajectories;

6) By varying the initial state of the asteroid's impact trajectories at t_0, we will obtain several sets of trajectories with given perigee distances r_π from the accepted range (1). The perigee distance r_π of close approach in 2036 is considered as a function of the initial state. Then, unlike in our previous works [6–9], in this stage, two directions are chosen – along the gradient of the energy constant and the opposite one:

$$x_1 = grad_{(r,v)}(h_0),\ x_2 = -grad_{(r,v)}(h_0)\,. \tag{4}$$

Along these directions, we find zero roots of the function $f_i = r_\pi(r_0,\ v_0) - c_i$, where c_i is the required magnitude of r_π.

Figure 2 shows a set of impact trajectories (~5000) in 2036 in the background of the dispersion region of the initial state (2) in the projection onto the (dr, dv) plane, where dr=r–r_n, dv=v–v_n.

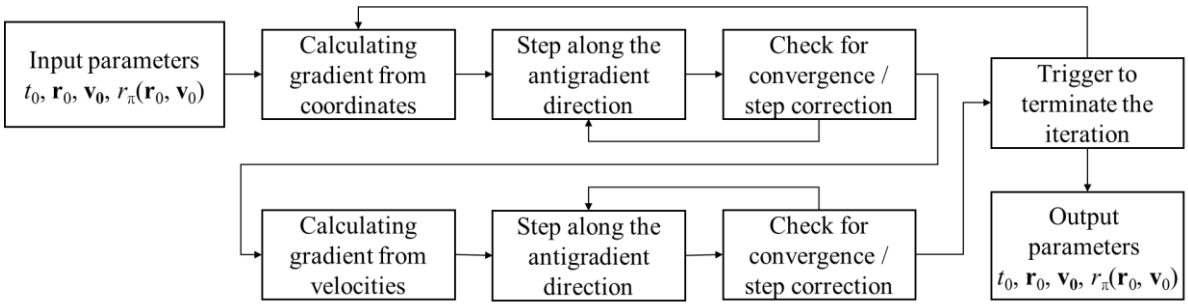

Figure 1. Flowchart to search for one impact trajectory by the gradient descent method

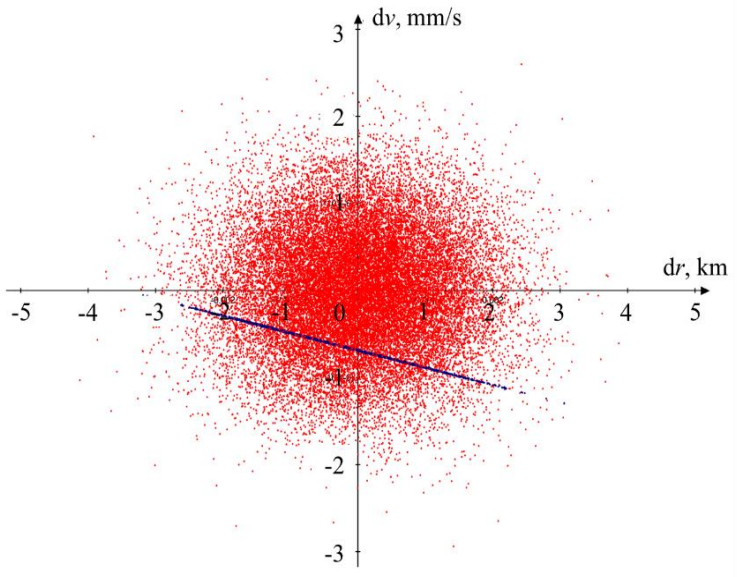

Figure 2. Dispersion region of the initial state and a set of impact trajectories (~ 5000) in 2036 on the (dr, dv) plane

According to computations [7, 9, 14], the minimum geocentric distance r_π for the 2036 encounter of the asteroid Apophis was estimated at about $r_{\pi\min}$~2070 km. These analogous results indicate the stability of the structure of potential collisions [14]. Therefore, to investigate further the characteristics of Apophis' impact trajectories, we have obtained several sets of impact trajectories with the geocentric distance r_π changing from the minimum distance $r_{\pi\min}$ to the Earth's radius. For each trajectory, we also have obtained position and velocity at the epoch when passing perigee in 2036:

$$t_\pi,\ \mathbf{r}_\pi(x_\pi,\ y_\pi,\ z_\pi),\ \mathbf{v}_\pi(v_{x\pi},\ v_{y\pi},\ v_{z\pi}). \tag{5}$$

3. Analysis of the characteristics of the asteroid Apophis' collision trajectories and the impact path of risk

3.1. Determination of the impact positions for Apophis

Next, we determined geographical coordinates of the impact points on the Earth's surface. As the geometric model of the Earth, we applied the model of a rotational ellipsoid around its minor axis with equatorial radius R_e = 6378.137 km and ellipticity α=1/298.25. Note that the influence of atmosphere, Earth's nutation and precession on the impact positions of the asteroid has not been taken into account. An analysis shows that the structure of the impact path on Earth changes slightly, the impact points move approximately towards east 40–60 km due to nutation and precession.

By numerical integrating the equations of motion of the asteroid described in 2.1 with the initial condition (5), we obtained the radius vector **r**, the "absolute" velocity vector **v** of the asteroid at any epoch *t*, and then transformed them to the Greenwich geocentric geoequatorial coordinate system, got the geocentric latitude φ_g and longitude λ_g, altitude *H* of the asteroid. Finally, taking into account the current time *t* and the Earth's oblateness, we calculated the geographical latitude φ and longitude λ of the asteroid's position [21–23].

We consider that the asteroid impacts the Earth when *H*=0. Let's denote respectively the time of collision, the latitude and longitude of the impact point by t_c, φ_c and λ_c. When *H*=100 km, the asteroid passes through the space-atmosphere boundary. The time of entry into the atmosphere is denoted as t_{atm}. Taking into account the angular velocity of the Earth's rotation, we also determined the relative velocity of the asteroid $\mathbf{v}_r$ with respect to the Earth's surface. As *H*=0, we computed absolute and relative velocities $\mathbf{v}_C$ and $\mathbf{v}_{Cr}$ at the collision point, velocity $\mathbf{v}_{\eta\zeta}$ is the projection of the relative velocity $\mathbf{v}_{Cr}$ on the Earth's surface. As *H*=100 km, we determined angles of inclination for the absolute and relative velocities to the horizontal plane, i.e. angles of entry into the atmosphere θ_a and θ_r.

3.2. Asteroid Apophis' path of risk

Several sets of the collision trajectories A_n (n=0, 1, …, 9), B_n (n=1, 2, …, 10), for each of which the perigee distance varies within certain ranges: (A_0)={r_π: 2069÷2100 km}, (A_1, B_1)={r_π: 2500±1 km}, (A_2, B_2)={r_π: 3000±1 km}, (A_3, B_3)={r_π: 3500±1 km}, (A_4, B_4)={r_π: 4000±1 km}, (A_5, B_5)={r_π: 4500±1 km}, (A_6, B_6)={r_π: 5000±1 km}, (A_7, B_7)={r_π: 5500±1 km}, (A_8, B_8)={r_π: 6000±1 km}, (A_9, B_9)={r_π: 6360±1 km}, (B_{10})={r_π: 6375±1 km}. The difference between A_n and B_n will be explained below.

Figure 3 shows the impact area A_0 on the plane of geographical angles (φ, λ) for the set of impact orbits with minimum perigee distances r_π in the range [2069, 2100] km. A cross marks its center. This area is located in the Pacific, between the west coast of the United States and Hawaii. It can be seen that only part of the area A_0 is connected as 2069 km≤r_π≤2085 km. When r_π>2085 km, impact areas on the Earth's surface for other sets of orbits {r_π=const} are divided into two subsets: one corresponds to a decrease of the heliocentric energy *h* before the collision, the other – increase of the heliocentric energy *h*, comparing with the energy of orbit with minimum perigee distance $r_{\pi\min}$.

Next, we displayed impact positions of all sets of trajectories A_n (n=1, ..., 9) and B_n (n=1, 2, ..., 10) on the Earth. They generate the Apophis' impact path of risk in 2036 (figure 4). Note that due to the non-sphericity of the Earth and the inclination of the trajectories to the equator, the Earth's radius on the

centers of areas A_9 and B_9 is different, about 6364 km for A_9 and 6376 km for B_9. Trajectories from A_9 almost touch the Earth's surface. However, trajectories from B_9 noticeably cross the Earth. So we added the set of orbits B_{10} with r_π=6375±1 km.

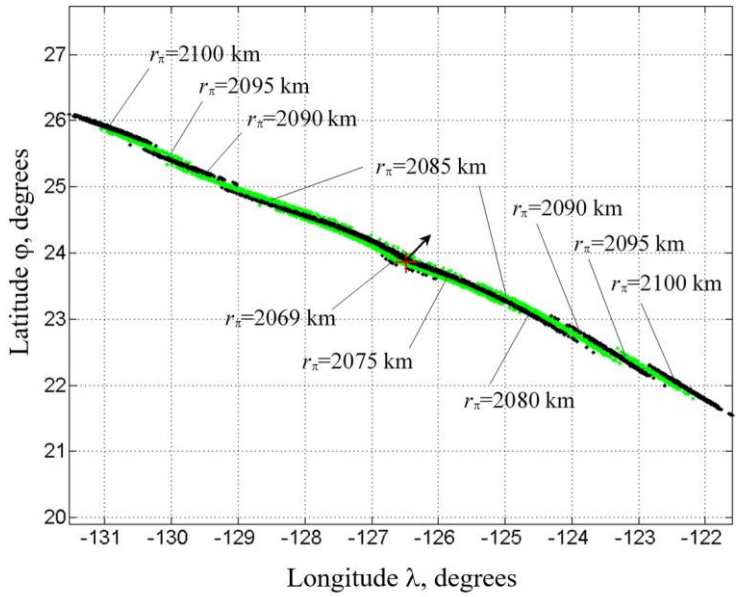

Figure 3. Impact area A_0 of the asteroid (99942) Apophis with minimum perigee distances $r_\pi \in [2069, 2100]$ km

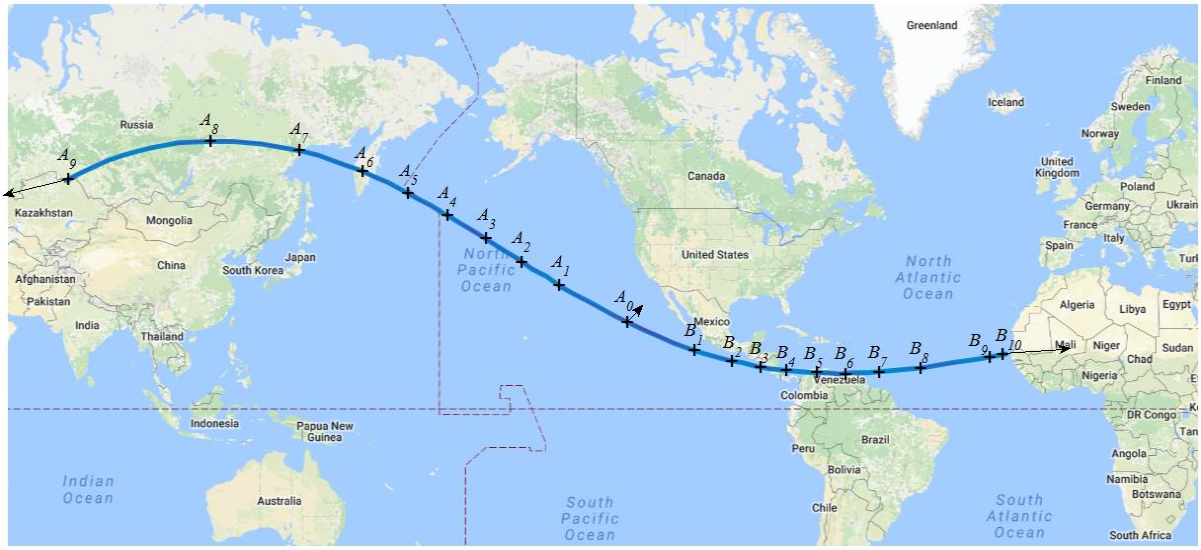

Figure 4. Asteroid (99942) Apophis' path of risk in 2036

The impact path of risk of Apophis lies in the Northern Hemisphere of the Earth. Its starting western point (area A_9) is located near Omsk, Tomsk, and Novosibirsk. Then it passes sequentially through the Krasnoyarsk region, Yakutia, the Far East, and Kamchatka of Russia, near the Aleutian Islands, across the North Pacific, Central America (Nicaragua, Costa Rica), South America (Colombia, Venezuela), ending in the Atlantic, just before reaching the west coast of Africa (near Dakar, area B_{10}), see figure 4. This path of risk is also given in [3, 4, 10, 12, 17]. Comparison of results by other authors with our ones, given here and in [10], shows that they almost completely coincide.

Numerical analysis has indicated that Apophis' path of risk lies approximately on a plane, and it is almost parallel to the ecliptic plane at collision epoch. We estimated the length and width of the PoR on the Earth's surface. In this case, we assumed approximately that the intersection of the PoR plane and the Earth is about a circle, its radius $R_P \approx 5370$ km. The central angle of PoR around the Earth $\phi \approx 4.534$ rad =259.8 degrees, then its length $L_P \approx \phi\, R_P = 24347$ km. The width of PoR was computed numerically according to the coordinates of the collision points in the normal direction to the longitudinal axis of PoR. The width of area A_0 is estimated at about 27 km. For A_i and B_i ($i \geq 1$), they are about 10–22 km wide. On average, the width of PoR is about 20 km. Note that in [17, 18], it was estimated at 30–50 km.

3.3. Characteristics of Apophis' collision trajectories

Figure 5 shows some temporal, energy, and geometric characteristics of the collision trajectories in the centers of all impact areas A_n and B_n. The impact area A_0 with the minimum perigee distance $r_{\pi\min}$ is located approximately at the center of this path of risk. For each set of trajectories (A_n, B_n) with 2085 km$<r_\pi<$6364 km, we obtained two areas, which are approximately symmetrical referring to the center of area A_0, areas A_n are at the west and B_n are at the east side of A_0, see figure 4. Areas A_n are generated by the orbits of the asteroid with higher energy before collision than in A_0, $h \in [-799.7689, -799.7554]$ km^2/s^2, here the semi-major axis of the Apophis orbit (7:6 exterior Earth resonance) $a \in [a_0, a_0+2784]$ km, $a_0 \approx 165938501$ km, see curve $h(\lambda)$, fig. 5. Areas B_n are generated by orbits with lower energy, $h \in [-799.7824, -799.7689]$ km^2/s^2, $a \in [a_0-2817, a_0]$ km.

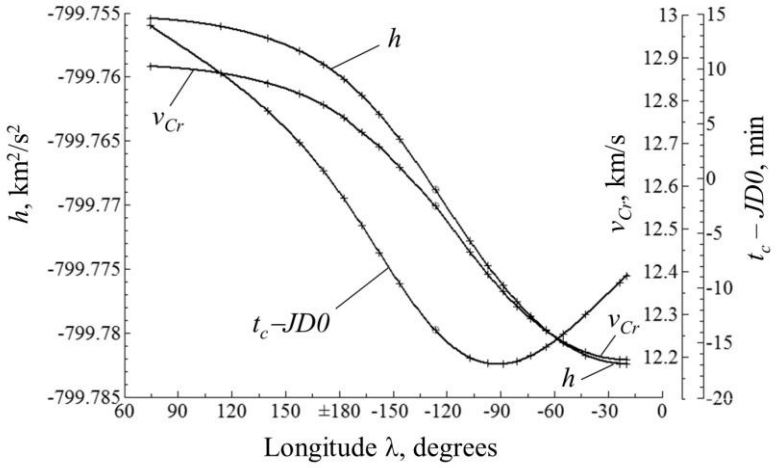

Figure 5. Dependence of relative impact speed v_{Cr}, energy before collision h and impact time t_c on the longitude of impact areas λ

Fig. 5 also shows the collision time t_c with respect to the reference time $JD0 = 9^h$, April 13, 2036=JD 2464796.875, this is about the mean collision time. For the whole set of trajectories, time t_c is in the range from $JD0$–17 min to $JD0$+13.8 min, see fig. 5, curve $t_c - JD0$ (λ). The absolute speed of collision with the Earth for Apophis is $V_{ca} \approx 12.6$ km/s, also in [4–10]. The rotation of the Earth leads to an increase of the collision speed at the west side of path of risk to ~ 12.9 km/s and to a decrease at the east side to ~ 12.2 km/s, see fig. 5, curve v_{Cr} (λ). In figure 4, the relative velocity vectors $\mathbf{v}_{\eta\zeta}$ in A_9, A_0 and B_{10} are shown. They correspond to the directions of the asteroid approach to the Earth.

Fig. 6 shows the angle of entry into the atmosphere θ_r, $\Delta\theta = \theta_a - \theta_r$, as well as the mean value of the perigee distance r_π of the impact areas A_n and B_n depending on the longitude λ. The largest magnitude of θ_a and θ_r is about 59°, this is in the area A_0. With increasing r_π, it decreases to about 8° in A_9, B_{10}. The difference between θ_a and θ_r is less than 1.5°, see the curve $\Delta\theta$ (λ) in fig. 6.

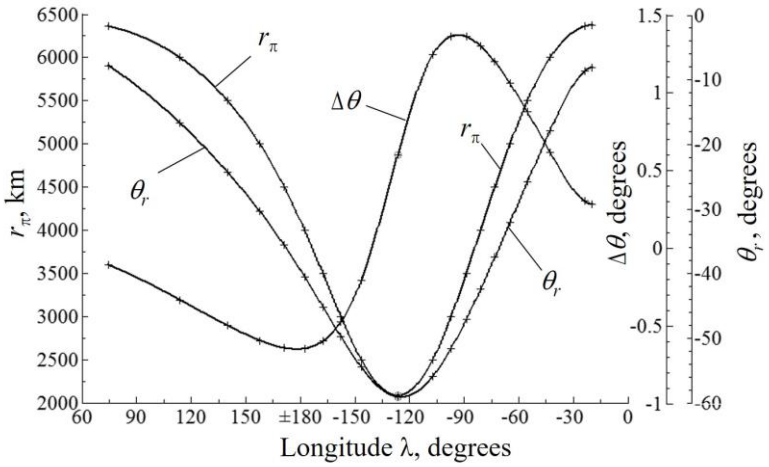

Figure 6. Dependence of the angle of entry into the atmosphere θ_r, $\Delta\theta=\theta_a-\theta_r$ and perigee distance r_π on the longitude of impact areas λ

3.4. Qualitative analysis of Apophis' close approach in 2036

The consideration of the target vector **b** in the B-plane and the velocity vector "at infinity" $\mathbf{v}_\infty$ of the hyperbolic geocentric orbits of Apophis helps to understand better the qualitative features of the set of Apophis' impact orbits. Numerical analysis has shown that for all collision orbits of Apophis, the endpoints of **b**-vectors, put aside from one starting point, form almost a line *L*, the direction vector of which is $\boldsymbol{S}=[-0.2443, 0.8776, 0.4124]^T$. Vectors $\mathbf{v}_\infty$ are almost constant and form an essentially plane passing through *L*, and then going to the plane of the PoR. The average value of vectors $\mathbf{v}_\infty$ is $\mathbf{v}_\infty=[5.5849, 0.7923, 1.6077]^T$ km/s, $|\mathbf{v}_\infty| = 5.87$ km/s, also in [2, 4]. For all orbits from A_0, the **b**-vector has an average magnitude $\mathbf{b}_0=[-1324.5, -3366.8, 6262.1]^T$ km, $|\mathbf{b}_0|= 7232$ km.

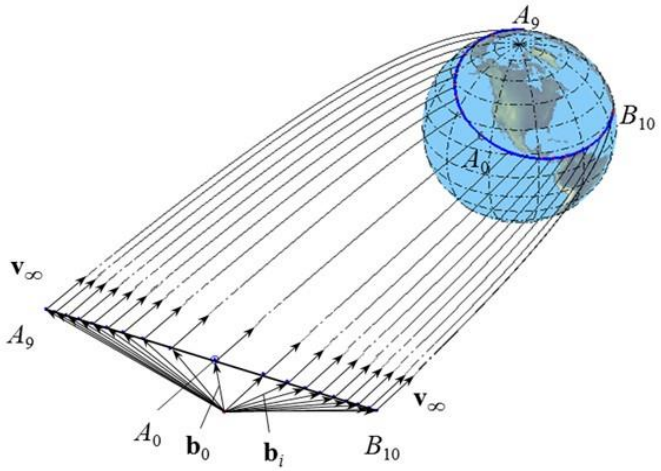

Figure 7. Possible impact trajectories of the asteroid Apophis in 2036

Figure 7 shows the geocentric motion of Apophis for all sets of impact trajectories in 2036. The velocity vectors "at infinity" and the **b**-vectors, as well as the possible impact path on the Earth's surface are shown in this figure. Isoline (contour line) $r_\pi=const$ will be approximately perpendicular to their corresponding target vectors **b**. Thus, as $r_\pi \approx r_{\pi\min} \approx 2069$ km, the isoline $r_\pi= const$ on the Earth's surface will be an arc along the longitudinal axis of PoR, which is shown in figure 3, and

approximately perpendicular to vector $\mathbf{b}_0$. With increasing $r_{\pi i}$, the inclination of the isoline $r_{\pi i}=const$ to the longitudinal axis of the PoR increases monotonically, and these isolines, being almost perpendicular to the vector $\mathbf{b}_i$, become almost perpendicular to the longitudinal axis of the PoR on its edges, for A_9 and B_{10}, see figures 3, 4 and 7.

4. Conclusions

Algorithms for searching all probable impact trajectories, for determining the coordinates of the intersection points of the Apophis' orbits with the Earth's surface and for constructing the impact area on the Earth have been developed. We have obtained a set of collision orbits with the Earth in 2036 for the asteroid Apophis and several probable sets of asteroid's trajectories, corresponding to the magnitude of the perigee distance of the Apophis' orbit from minimum distance of about 2070 km to the Earth's radius. The possible impact areas, i.e. the Path of Risk of the asteroid Apophis in 2036 have been constructed on the Earth's surface. There have been studied the geometric, temporal and energy characteristics of the Apophis' collision trajectories and the Path of Risk, in particular, its width and length, the angle of the asteroid's entry into the atmosphere, time and the speed of collision, the direction of the approach of the asteroid to the Earth. Comparison of our results with other works on this issue shows that they coincide well.

References

[1] Yagudina E I and Shor V A 2005 *All-Russian Conf. "Asteroid-Comet Hazard-2005 (ACH-2005)"* (St. Petersburg, Oct. 3–7 2005) pp 355–358
[2] Chesley S R 2006 *Proc. 229th IAU Symp. 2005* (Cambridge Univ. Press) pp 215–228
[3] Russell Schweickart, C Chapman, D Durda, P Hut, B Bottke and D Nesvorny 2006 Threat Characterization: Trajectory Dynamics (White Paper 39) *B612 Foundation*
[4] D B Gennery 2007 Scenarios for dealing with Apophis *Plan. Def. Conf.* (G. Wash. Univ. USA, Mar. 5–8 2007)
[5] Giorgini J D *et al* 2008 *Icarus* **193** pp 1–19
[6] Ivashkin V V and Stikhno C A 2007 An analysis of the correction problem for the near-Earth asteroid (99942) Apophis-2004 MN4 *Plan. Def. Conf.* (G. Wash. Univ. USA, Mar. 5–8 2007)
[7] Ivashkin V V and Stikhno C A 2007 A problem of the orbit correction for the near-Earth asteroid Apophis *58th Inter. Astron. Cong.* (Hyderabad, India, Sep. 24–28 2007)
[8] Ivashkin V V and Stikhno CA 2008 *Dokl. Akad. Nauk* **419**(5) pp 624–627
[9] Ivashkin V V and Stikhno C A 2009 *Sol. Syst. Res.* **43**(6) pp 502–516
[10] Ivashkin V V, Stikhno C A and Guo P 2017 *Dokl. Phys.* **62**(8) pp 387–391
[11] Włodarczyk I 2008 *Contrib. Astron. Obs. Skalnate Pleso* **38** pp 21–32
[12] Włodarczyk I 2010 *Proc. Int. Conf. "Asteroid-Comet Hazard-2009"* (SPb.: Nauka) pp 299–301
[13] Włodarczyk I 2013 *Mon. Not. R. Astron. Soc.* **434** pp 3055–3060
[14] Sokolov L L *et al* 2012 *Sol. Syst. Res.* **46**(4) pp 291–300
[15] Sokolov L L, Borisova T P, Vasilev A A and Petrov N A 2013 *Sol. Syst. Res.* **47**(5) pp 408–413
[16] Sokolov L L, Kuteeva G A 2015 *Vestn. St.Petersb. Univ. Ser.* **2**(60) pp 148–156
[17] https://en.wikipedia.org/wiki/99942_Apophis
[18] http://galspace.spb.ru/index129.html
[19] https://en.wikipedia.org/wiki/B612Foundation
[20] Stepan'yants V A and L'vov D V 2000 *Math. Model.* **12**(6) pp 9–14
[21] Akim E L and Eneev T M 1963 *Cosm. Res.* **1**(1) pp 5–50
[22] Kaplan G H 2005 The IAU resolutions on astronomical reference systems, time scales, and Earth rotation models. Explanation and Implementation *US Naval Obser. Circular №179 Wash. DC* 20392 p 118
[23] Vallado David A 2007 Fundamentals of astrodynamics and applications 3rd ed. *Sp. Tech. Lib. Springer NY.* vol 24 p 1055